Synthetic Strategies for (Supported) Metal and Metal Oxide Catalysts: Case Studies

Chapter 6

Synthetic strategies for metal and metal oxide (supported) catalysts: case studies

Abstract

As outlined in previous chapters, the sol-gel method, which originated around the preparation of silica, has developed massively over time, generating a plethora of different methodologies and chemistries. This inexhaustible source of synthetic pathways has been a powerful tool at the research community's disposal to prepare increasingly advanced catalytic formulations. Nevertheless, by using more sophisticated chemistry compared to conventional synthesis methods, challenges can be encountered in obtaining the desired products. These can be overcome by adopting the appropriate strategies and selecting the most suitable route bearing in mind the final composition and required properties. The optimal way to understand how to approach this subject in order to design reliable and sustainable syntheses that allow the control of composition, structure and surface properties, is to exploit some case studies. The selected examples cover some of the main fields of application of metal and oxide supported catalysts in heterogeneous catalysis.

Keywords: acid catalysts, supported metal catalysts, reverse micelles approach, photocatalysts

6.1 Acid catalysts

- P_2O_5-SiO_2

Oxide-based systems containing P_2O_5 have been the subject of considerable interest in the field of sensor chemistry due to their high proton conductivity [1-4]. In particular, phosphosilicate glasses have proven to be excellent candidates as sensing elements in integrated humidity sensors. The need to understand the conduction mechanism and to identify the role and contribution of surface hydroxyl groups and phosphorus distribution within the silica matrix has promoted extensive research on these materials using complementary characterization techniques, among which nuclear magnetic resonance has played a primary role.

The authors [5,6] performed ^{1}H MAS-NMR spectroscopy with ^{1}H T_1 and $T_{1\rho}$ relaxation times as well as low-temperature ^{1}H solid-echo NMR on gels of composition $10P_2O_5$-$90SiO_2$ and $30P_2O_5$-$70SiO_2$ to correlate differences in proton conductivity with the size of phosphorus domains. A uniform distribution of small POH domains that give rise to dynamic processes was showed only by the sample with a high phosphorus content. As evidence of this, a single narrow ^{1}H resonance connected to the POH groups was shown. The sample with the lowest phosphorus content heat-treated at 400 °C present an inhomogeneous distribution of POH groups, not allowing a proton hopping pathway to be formed. More recently, Esposito et al. [7] used an extrinsic probe, the muon, to further investigate the mechanism of proton conductivity in phosphosilicate gels. The work explored both the nature of the sites involved and the proton dynamics using muon spin relaxation. Another peculiar feature of silicophosphates is the formation of hexacoordinate silicon in certain crystalline phases, including $Si_5O(PO_4)_6$, $Si_3(PO_4)_4$ and SiP_2O_7. A reproducible synthesis of silicophosphates could also be complicated by the existence of numerous polymorphs of crystalline silicon diphosphate with octahedrally coordinated silicon [8-10].

With regard to catalysis, the presence of Brønsted acid sites makes silicophosphates valuable materials for acid catalysis [8,11]. A significant number of processes in the petrochemical industry requires the use of acid catalysts, which, depending on the type of reaction, must feature Brønsted or Lewis sites with a certain strength [12,13].

Although they are widely used in hydrocarbon processing reactions, there is much interest in the development of advanced active and low-cost formulations for the transformation of biomass into value-added products. A great deal of effort is devoted to the production of green products through the use of renewable resources to improve environmental impact. Efficient conversion pathways, such as hydrolysis of cellulose, dehydration of saccharides, acetylation, alkylation, and acylation, are catalysed by acids. environmentally friendly chemical processes [14].

In this scenario, design of solid acid catalysts has a central role to establish environmentally friendly catalytic processes. A basic task of the present review is the pivotal role of the synthesis route to consciously tailor the features of the final product to comply with the requirements of the catalytic reaction.
The first bottleneck encountered in the synthesis of silico-phosphates by the conventional hydrolytic method is the choice of silicon and phosphorus precursors. While the choice of silicon precursor seems obvious, considering the well-known sol-gel chemistry of TEOS, the exact choice of phosphorus precursor can be critical and dramatically affect the extent of copolymerization between silicate and phosphate units, the type and the relative amount of crystalline phases, the final composition and the textural and surface properties. [15]. Phosphates and silicates have similar crystal structures, consisting of tetrahedral $[PO_4]_3$ and $[SiO_4]_4$ units, respectively. Despite this, the reactivity of TEOS can be increased with acidic or basic catalysis whereas drastic conditions, such as heating under reflux for prolonged times, result in only partial hydrolysis of the triethylphosphate $PO(OEt)_3$. The homo-condensation of the silanol groups is thus favoured and the silica fraction grows around the phosphorus precursor mostly present in monomeric form [15-17]. Phosphorus-containing molecules trapped and weakly interacting with the silica matrix easily evaporate during heat treatment and the composition of the final product deviates from the nominal one. Furthermore, it is worth bearing in mind that the Si-O-P bond is sensitive to the presence of water, which easily causes its hydrolysis [18,19].
The effectiveness of the phosphorus precursor was revealed by in-depth studies of the structure of the silicophosphate gels, with particular reference to the extent of Si-O-P bond formation. Nuclear magnetic resonance in the liquid and solid state on the ^{1}H, ^{31}P and ^{29}Si nuclei was decisive in establishing that, after 10 months, phosphorus was still only present in the pristine alkoxide TEP (triethylphosphate $PO(OEt)_3$) [20]. In the same study, Schrotter et al. revealed how the use of alternative precursors to TEP, namely $P(OEt)_3$ and $(OEt)_2P–O–P(OEt)_2$, led to complete hydrolysis to phosphoric acid via intermediate species. However, rapid and uncontrolled hydrolysis could cause precipitation or the formation of inhomogeneous gels. Furthermore, different crystallisation behaviour was observed by varying the phosphorus precursor, with quite controversial results, probably due to the Si/P ratio and the adopted synthesis route. Szu at al. [21] obtain amorphous gels even after prolonged treatment at 800 °C using TEP. Conversely, Matsuda et al. [22] observe crystallisation of tetragonal and monoclinic SiP_2O_7 in gels calcined at 450 and 600 °C. There is a quite large numbers of paper reporting attempts to prepare cross-linked Si–O–P inorganic network using phosphoric acid as precursor. As mentioned above, the major concern arises from its very rapid hydrolysis compared to the silica precursor. However, the presence of monomeric or dimeric units containing POH groups leads to greater interaction with the silica matrix and, therefore, less P losses during heat treatment compared to preparations with TEP [21-23]. Still within the hydrolytic route, Esposito et al. reported an intriguing synthetic strategy that overcomes the obstacles encountered with the phosphorus precursors mentioned above. The authors succeed in obtaining gels with 10 and 30 mol % of P_2O_5 without loss of phosphorus, avoiding time-consuming steps and drastic operating conditions [9,18]. The adopted approach entails the use of phosphorus oxychloride, $POCl_3$, whose reactivity is controlled by replacing part of the chlorine atoms with OR groups. $POCl_3$ is mixed with anhydrous ethyl alcohol in a 1:6 molar ratio obtaining $POCl_31\text{-}x(OEt)x$ species bearing a reduced partial positive charge on phosphorus compared with the initial precursor. MAS-NMR characterization provides evidence that the degree of Si-O-P cross-linking is closely dependent on phosphorus content, while the temperature of heat treatment may contribute to the self-condensation of POH groups. Evidence of Si-O-P bond formation in the gel containing 30 mol% P_2O_5 is provided by the ^{29}Si resonances at -211 and -215 ppm, which are characteristic of six-coordinate silicon in phosphosilicates.
An equally fascinating approach is that proposed by Styskalik et al. [8] They obtain an inorganic Si-O-P cross-linked network featuring surface residual organic groups by selecting a nonhydrolytic ester elimination pathway. The degree of Si-O-P condensation can be handled through the synthesis parameters, such as solvent, temperature and reaction time. Conversely, formation of trapped oligomeric phosphorus species is not observed. This procedure, in its optimized condition, produces xerogels with remarkable surface area.

- <u>Ru-Nb_2O_5-SiO_2</u>

A worldwide matter of concern that has a dramatic environmental and social impact is the growing demand for energy and the urgent need for renewable resources. Currently, biomass-based energy system is the most reliable option to diminish reliance on fossil fuels through the development of green and sustainable

chemistry. One of the main benefits of biomass-based fuel (sometimes called as biofuel) is zero carbon dioxide release as compared to fossil fuel, not contributing to the global warming [24].
In addition, biomass has a high potential for the production of value-added products that drive the research community to constantly search for valuable and sustainable reaction pathways [25].
From this point of view, a notable example of biomass valorisation is represented by the hydrogenation of levulinic acid (LA) into γ-valerolactone (GVL), Figure 6.1.

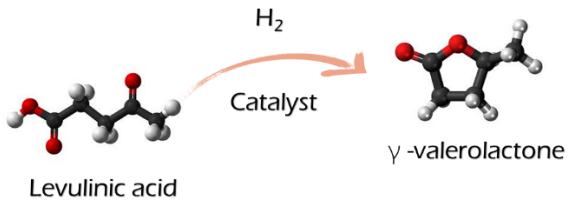

Figure 6.1 Hydrogenation of levulinic acid

The levulinic acid can be considered a valuable and versatile molecule for the production of renewable fuels, fuel additives, green solvents, polymers, value-added fine chemicals, flavouring agents and resins. Actually, LA grabs the industrial interest because it possesses both keto and carboxylic acid groups and it can undergo a series of chemical reactions such as esterification, hydrogenation, halogenation, and oxidation. However, to highlight the value of LA, the most promising reaction is the hydrogenation to γ-valerolactone (GVL), a green platform molecule that has gained considerable attention in the last decade [26-28]. The reaction pathway of levulinic acid to GVL at low temperature can be described by a first step of hydrogenation to γ-hydroxypentanoic acid (HPA) followed by a second step in which intramolecular lactonisation to GVL occurs [29,30].
A literature survey of the aqueous-phase hydrogenation of biosourced molecules shows that ruthenium metal particles supported on various carbons and oxides were the most efficient catalysts to achieve a rapid and selective conversion of carbonyl functionalities into the corresponding alcohols. This type of mechanism highlights the need for catalysts characterised by a dual redox-acid functionality.
Ru/C, being characterised by the presence of both metal and acid sites, is the commercial catalyst commonly used for this reaction, but it has the non-negligible inconvenience of a slow but irreversible deactivation, probably due to the sintering of the ruthenium particles and the formation of carbon deposits on the surface of the catalyst [31].
Furthermore, the authors [30] point out that the yield at GVL can be significantly increased by using an acidic co-catalyst, such as commercial niobium phosphate ($NbOPO_4$, NBP) or niobium oxide.
This implies that the process can be further optimised with the use of a ternary system containing both functionalities. The preparation of a ternary system by the wet route could be rather complicated, as the design of the synthesis route should consider the different chemistry of the precursors.
To prepare a bifunctional catalyst, Sun et al. [32] followed a wet chemistry route using H_3PO_4 and $NbCl_5$ as precursors for the acid fraction. They succeeded in obtaining a mesoporous niobium phosphate using a structure directing agent P123 through a somewhat time-consuming multistep procedure with a double autoclave treatment initially at 313 K and subsequently at 348 K. The fraction with redox properties consisting of Ru particles is embedded by adsorption of colloidal Ru nanoparticles on solid acids. The colloidal Ru nanoparticles were prepared by the reduction of $RuCl_3$ with ascorbic acid in a suitable solvent. The autoclave time, the type of solvent and the temperature proved to be useful parameters for tailoring the size of Ru NPs.
Rather than anchoring or trapping ruthenium in the acid matrix, the authors [29,31] developed a one-step procedure by operating with a reaction environment containing both niobium and silicon precursors. The purpose was to guarantee significant dispersion of the ruthenium nanoparticles for an active and stable catalyst.
Niobium chloride was mixed with ethyl alcohol to control the rate of hydrolysis, obtaining less reactive species, $Nb(OEt)_{5-x}(Cl)_x$. This idea echoes the one devised for the precursor $POCl_3$ in the preparation of silico-phosphates, *vide supra*. The solution containing niobium was mixed with an alcoholic solution of TEOS containing a certain amount of $RuCl_3 \cdot 3H_2O$. A dark gel was obtained by dropwise addition of water to a final

H_2O/TEOS ratio equal to 4/1. The procedure is efficient, requiring few and simple steps, without the use of elaborate equipment and conducted at room temperature.
The obtained catalysts can be described as mixed oxo network of niobium and silicon in which ruthenium was uniformly dispersed, avoiding segregation. Notable surface area (between 400 and 500 m^2g^{-1}) were obtained without any surfactant. Catalysts containing Ru NPs are obtained through a reduction pre-treatment in H_2. While ruthenium effectively hydrogenated LA to HPA, the subsequent lactonisation reaction was promoted by the presence of niobium oxide, which was responsible for the increased acidity of the catalyst. Finally, cyclic tests have proven the stability of the catalysts [29,31].

6.2 Highly dispersed supported metal catalysts

- Co-SiO_2

Cobalt-based catalysts play a starring role in the field of heterogeneous catalysis [33-39]. They can offer comparable or even better performance than noble metals, with the considerable advantage of being more affordable. In oxidised form, they are successfully used in the oxidation reactions of organics [33]. A reaction with a strong environmental impact is the oxidation of volatile organic compounds, VOCs, whose presence is harmful to air quality and human health. The origin of VOCs emissions is diverse, including mobile sources in urban settings and manufacturing and processing industries [34,35]. Mixed valence cobalt oxide, Co_3O_4, is extensively reported as the most active metal oxide for total oxidation [36,37].
The redox chemistry of cobalt, $Co^{3+} \leftrightarrow Co^{2+} \leftrightarrow Co$, hence the cobalt species that are formed and their interaction with the support represent a crucial point in the design of a material with high performance. For this reason, a big effort has been spent to tailor the materials features through the variation of the synthesis parameters [38].
Cobalt oxide chemistry is characterized by two stable oxides, CoO and Co_3O_4, being the latter the most stable at room temperature. Co_3O_4 can be described as a mixed valence oxide, (AB_2O_4), where the Co^{2+} ions occupy A sites with tetrahedral (Td) symmetry, while those in the B sites with octahedral (Oh) symmetry are trivalent (Co^{3+}) [40]. In wet chemical methods, Co^{2+} salts are generally used because $[Co(H_2O)_6]^{2+}$ is stable in aqueous solution. Conversely, $[Co(H_2O)_6]^{3+}$ is a strong oxidising agent and in aqueous solution, unless acidic, it rapidly decomposes by oxidising water with oxygen evolution. Consequently, unlike Co (II), Co (III) provides few simple salts and those obtained are unstable. B. Puértolas et al. [41] used a modified Pechini method to prepare unsupported Co_3O_4 as a catalyst for the total oxidation of propane. Cobalt II nitrate and organic acids (glyoxylic acid or ketoglutaric acid) were employed in the synthesis. Despite the simplicity of the procedure, the method proved ineffective in achieving an improvement in catalytic activity compared to the reference catalysts. The low surface area was considered the main factor negatively affecting catalytic performance.
To improve textural and structural properties without involving too complex and difficult operations, cobalt oxide is generally dispersed on a porous support, with an increase in the number of active sites.
SiO_2 is one of the most attractive media on account of its versatility, tailorable porosity, excellent chemical and thermal stability and, not least, because it can be easily surface-modified with organic groups allowing the anchoring of specific catalytic centres. In addition, the type of silica morphology and texture can drive the formation of specific Co phase(s) and also affect the cobalt oxide particles size and their distribution in silica structure [42,43].
An intriguing and fascinating approach to shed light on the relationship between structure and activity of silica-supported cobalt oxide in the catalytic oxidation of carbon monoxide was reported by Eurov et al. [43]. They prepared a series of silicas with different pore structures using a sol-gel approach, following the protocol described in Figure 6.2. Mesoporous silica particles were obtained by hydrolysing TEOS in a hydroalcoholic solution in the presence of cetyltrimethylammonium bromide (CTAB) while micro-mesoporous SiO_2 particles with a pore size of 0.9-3.5 nm were synthesised using a modified silica precursor, 3-(methacryloxy)propyl]trimethoxysilane (MPTMOS), along with TEOS.
The particles were decorated with cobalt oxides using the capillary impregnation method. Cobalt is essentially found as Co_3O_4 located on the outer surface of the silica particles or as Co^{2+} interacting with the substrate inside the pores.

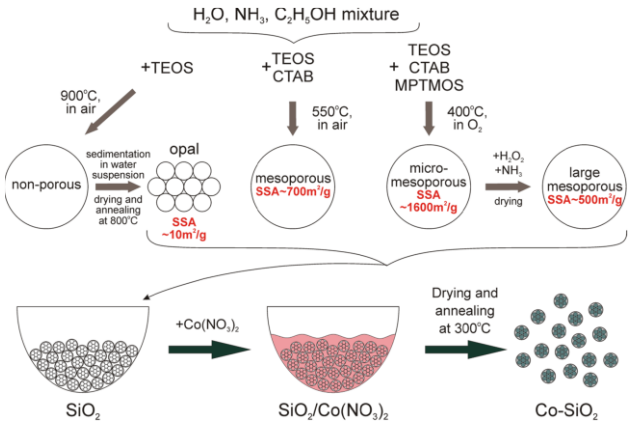

Figure 6.2 Schematic illustration of the Co-SiO_2 composites preparation. Adapted with permission from [43]; Copyright 2022 Elsevier.

Cobalt, in its oxidised form, has gained a distinctive position in one of the most significant processes in the field of renewable and clean energy resources, the oxygen evolution reaction (OER) [44]. In the work of Tüysüz et al [45], porous silicas were used as hard templates, taking the advantage of the nanocasting method, for the preparation of designed Co_3O_4 catalysts as electrocatalyst for water oxidation. In particular, cubic ordered mesoporous silicas, KIT-6, with different textural parameters, were used as a hard template to fabricate mesoporous ordered cubic Co_3O_4. The adopted strategy provided a catalyst with an open structure and a high surface area, which proved to be the pivotal factors in achieving remarkable activity. Mesoporous cobalt oxide also showed excellent structural stability during the electrolysis of water [45].

Cobalt is an efficient catalyst not only as a stable oxide but also in its metallic state. Indeed, there are processes, such as the Fischer-Tropsch synthesis for the production of liquid hydrocarbons from syngas, which require the catalyst to be activated by reduction treatments at a temperature above 350 °C in order to obtain the active phase Co^0.

In this case, mixed cobalt oxide is considered the precursor to metallic cobalt owing to its reducibility at low temperature, but, above a certain particle size, its formation is symptomatic of a low dispersion of cobalt species, which is detrimental to catalytic activity. On the other hand, increased interaction between the metal and the matrix can lead to a cobalt silicate phase that is hardly reducible [46,47].

Therefore, an effective synthesis design should allow the definition of new pathways driving the formation of specific cobalt phases by achieving the delicate balance between reducibility, dispersion and reactivity.

The use of surfactants in the supramolecular templating approach has been massively explored. For this reason, some strategies that make unconventional use of surfactants will be reported.

Recently, Olguin et al. [48] employed a short cationic surfactant, 3-hexyl triethyl ammonium bromide, at a concentration below the critical micelle concentration point (CMC), to prepare microporous cobalt oxide silica. They observed how the amount of the Co_3O_4 is tunable through the concentration of the quaternary ammonium surfactant. Indeed, at low surfactant amounts, the formation of $CoBr_x^{2-x}$ species in the xerogel facilitates the formation of Co_3O_4 during heat treatment. The reverse effect is observed with increasing surfactant due to interactions between the $CoBr_x^{2-x}$ species, the surfactant head groups and the silica surface. Keeping the cobalt precursor content unchanged, the authors also explored the effect of the carbon number of quaternary ammonium surfactants. The point at which the decrease in cobalt oxide occurs was found to be a function of the length of the alkyl chain of the surfactant. Quaternary ammonium salts with a longer chain cause an earlier transition to the formation of cobalt species more strongly interacting with the silica matrix. The pore size was also tailored by the increase in surfactant, with higher loading promoting mesoporosity.

Still working under conditions that circumvent amphiphile aggregation or micelle formation, the authors [42] explored a challenging route for the immobilization of highly dispersed cobalt species in the silica framework in high metal loading using a non-ionic surfactant.

The foremost task of this approach was to identify a single molecule acting both as a porogenic template to modify textural properties and as an oxygen-rich complexing agent for metal species. In this way, the dual

result of modifying textural properties while simultaneously acting on cobalt dispersion, even at high cobalt contents, can be attained. Following the procedure, the polyoxyethylene (10) cetyl ether, Brij C10, was added to a solution containing partially hydrolyzed Si(OR)x(OH)y and $[Co(H_2O)_6]^{2+}$ aquo-ion, Figure 6.3. TEOS was hydrolysed at 50 °C without any alcoholic solvent, by using concentrate HNO_3 as catalyst, in the following molar ratio TEOS : H_2O : HNO_3 = 1 : 4 : 0.01. The absence of an alcoholic solvent sets the system in the "immiscibility" state. However, as TEOS hydrolysis takes place with both water consumption and alcohol production, the system moves towards the miscibility region. This approach allowed high concentrations of hydro-soluble inorganic salts to be introduced into the reaction system. For comparison, the authors prepared the same compositions, CoOx-SiO_2 featuring 10 and 30 mol % Co, without using the surfactant. The pre-reduced catalysts were tested in the ethanol steam reforming reaction [42].

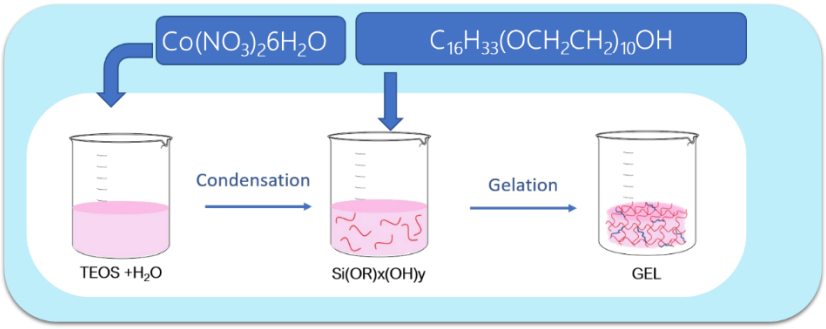

Figure 6.3 Non-Ionic Surfactant Assisted Sol-Gel route

The steam reforming of biofuels, such as ethanol, is an excellent opportunity to produce hydrogen from renewable sources [49]. The main challenge, as we have seen for the processes mentioned aforementioned, is the development of cost-effective catalysts with a high conversion efficiency, while limiting the use of noble metals. Several studies have recognised nickel and cobalt as very valuable alternatives due to their high C-C bond cleavage activity [50].
The overall ethanol steam reforming (ESR) reaction can be represented by Eq. (1), but this process involves several steps and reactions leading to the formation of by-products, such as carbon monoxide, methane, acetaldehyde or ethylene, which are also coke precursors.

$$CH_3CH_2OH+3H_2O \rightarrow 2CO_2+6H_2 \quad \text{eq (1)}$$

A suitable ESR catalyst must then meet stringent requirements, not only promote an increased conversion of ethanol into hydrogen, but also prevent possible undesirable reactions and limit cook formation.
Surfactant-assisted sol-gel synthesis has emerged as a viable strategy to deal with the redox chemistry of cobalt while simultaneously achieving outstanding surface area.
Notably, the chelating action of the surfactant substantially increased the fraction of reducible dispersed cobalt species in gels containing 10 mol % Co. At higher cobalt loadings, the surfactant pathway prevents Co agglomeration leading to finely dispersed species. Although reducible at higher temperatures compared to the segregated phase of Co_3O_4 obtained in the reference sample, they potentially produce the same amount of metallic cobalt [15].

- Cu-ZrO_2

Compared to natural gases, alcohols derived from biomass are undoubtedly fascinating sources for hydrogen production, as they are carbon-neutral. In particular, methanol features extremely attractive characteristics compared to alcohols with a higher carbon number. The absence of carbon-carbon bonds makes hydrogen extraction more feasible, with considerably lower operating temperatures than those required for ethanol steam reforming [51-52].

Although the selection of the best cost-effective raw material should be based on the overall economics of the process and the local government policies, methanol is highly recommended for its safe handling, low cost, high energy density and flexibility, being generated by from multiple sources [51]
Extensive research has been conducted over the years to find valuable and efficient alternatives to noble metals-based catalysts, with the aim of ensuring maximum activity and selectivity for higher hydrogen yield and lower CO production.
Copper-based catalysts have been identified as particularly promising in the steam reforming reaction though the literature clearly reveals that catalyst performance can be dependent on many cross-cutting factors such as composition, the presence of promoters, the nature and acidity of the support, and the physico-chemical properties often closely related to the adopted synthetic route.
The selection of the carrier is then of utmost importance because it can contribute decisively to the dispersion of the active phase and its availability. It can also improve selectivity towards the desired product and improve the stability of the catalyst itself. Compared to the more common Al_2O_3 and SiO_2 supports, ZrO_2 is of particular interest due to its weak acidity and basicity, its mechanical and thermal stability, and its redox behaviour [53-55].
Actually, Cu-ZrO_2 is not only a suitable candidate for steam reforming, it is a high-potential catalyst in a number of reactions concerning the production of liquid fuels and chemicals from renewable raw materials such as biomass [53, 55, 56]. Polymorphic transitions in oxides, like those occurring in zirconium oxide, can have a strong impact on surface properties and, consequently, on the amount and distribution of active sites. From this point of view, the most sought-after synthesis routes are those allowing the tailoring of the crystalline phase.
The preparation have to address some important key factors: metal dispersion, overall surface area and particles size. Well, despite the many advantages of the sol-gel procedure, the big issue when the preparation involves the transition metal alkoxides is their very fast reaction with water that lead to a precipitation instead of a homogeneous sol. As a consequence, there is poor control on composition and homogeneity.
Although the hydrolysis may be controlled by coordination with suitable ligands, the addition of a metal salt can further complicate the system because it might hinder, in some extent, the formation of Zr complexes.

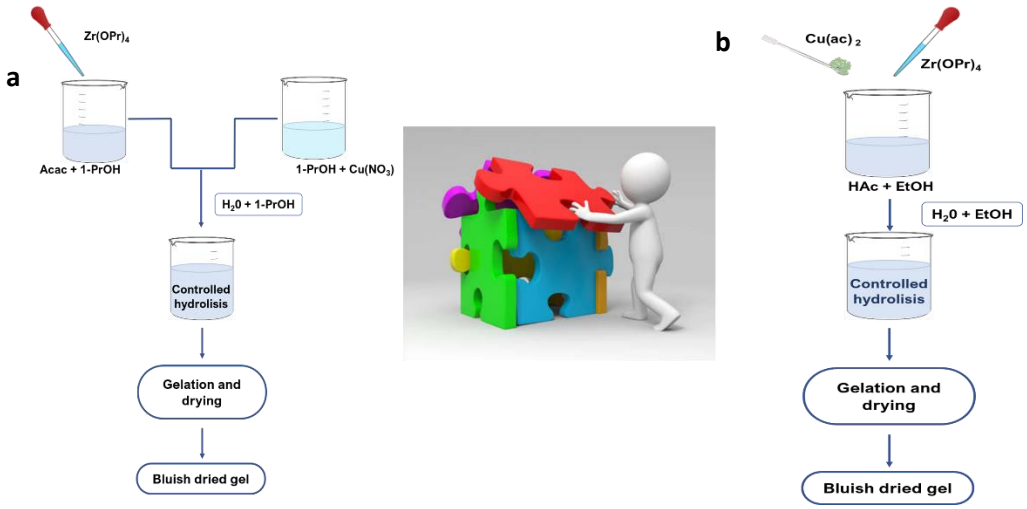

Fig 6.4 Flow chart of the hydrolytic sol-gel synthesis of CuOx-ZrO_2 by using a) acetylacetone and copper nitrate as copper nitrate or b) acetic acid and copper acetate.

The authors [53,54] designed two different sol-gel routes that successfully led to homogeneous polymer gels consisting of CuOx copper oxide dispersed in a zirconia matrix, Figure 6.4. The procedures were conceived based on two different copper precursors and two different approaches to control the hydrolysis of the zirconium precursor.
The high polarity of the Zr-O bond makes Zr alkoxides highly susceptible to nucleophilic attack. They can hydrolyse upon simple exposure to ambient moisture. In addition, coordination expansion is a general

tendency of zirconium alkoxides. It occurs spontaneously through solvation or oligomerisation and some zirconium alkoxides would present oligomeric molecular structures [57]. For these reasons, zirconium alkoxides must be stored in humidity-controlled environments and preparations of catalysts using zirconium alkoxides must be carried out in dry boxes.

In a first approach, the hydrolysis of zirconium(IV) propoxide, used as a precursor in all preparations, was thoroughly controlled with the use of acetylacetone. Acetylacetone, however, can also coordinate Cu^{2+} in solution thus reducing its efficacy as a chelating agent for Zr. This assumption is supported by the increased content of acetylacetone required for a stable sol, compared to the preparation of pure zirconia [54].

Copper nitrate hydrate, $Cu(NO_3)_2 \cdot 2.5H_2O$, used as a precursor, was added dissolved in 1-propanol to counteract the formation of a precipitate caused by the water included in the salt structure. Finally, water for hydrolysis was added in mixture with 1-propanol, and the best ratio to avoid the formation of insoluble oligomeric species was (1/1.9), Figure 6.4a. The bluish transparent gel obtained in 30 min can be described as a zirconia matrix obtained by polymerization of Zr(OPr)x(OH)y oligomers trapping copper species.

The use of acetic acid and a different copper precursor, in a second alternative route, has required the development of a new procedure, Figure 6.4b.

Acetic acid needs to be handled carefully as it possesses contrasting functionalities. On the one hand it can behave as an acid catalyst in the hydrolysis reaction promoting further precipitation, on the other hand its function as a bidentate ligand agent of Zr alkoxide is reported [58]. The role of acetic acid as a modifier of transition metal alkoxide through ligand exchange can further complicate the control of hydrolysis kinetics. All the above may interfere with the condensation pathway and with the whole process of sol formation [59-63]. The authors studied the effect of the HAc/Zr molar ratio on gel formation observing that a rapid reaction with water, with massive precipitation, occurred for an acid/alkoxide ratio of less than 1.6. The formation of a stable sol without limiting gel formation is ensured by a HAc/Zr ratio of two, in agreement with the results of other authors [15, 64]. The in-situ water source from the esterification reaction between acetic acid and ethanol explained the lower amount of added water compared with the acetylacetone preparation.

The preparation of copper zirconia catalysts is an example of the dramatic impact that the synthesis route can have on the performance of a catalytic material.

The first noteworthy result was the modification of the thermal behaviour induced by the synthesis procedure with a shift to higher temperature of the crystallization peak for the sample prepared by acetylacetone and copper nitrate [53, 54]. This important finding is related to the possible modification of the crystal lattice of zirconium oxide by copper impurities. This exclusively involves Cu^{2+} ions since Cu^{+} ions have an ionic radius much larger than the one of Zr^{4+}. In this phenomenon, the copper precursor played a critical role since nitrate promotes an oxidizing environment favouring the formation of CuO whereas acetate decomposes initially giving cuprous oxide, Cu_2O, as the main product.

The textural properties of the catalysts, obtained by reduction at 300 and 450 °C, were severely affected by the crystallization behaviour of the xerogels. Indeed, the materials prepared by acetylacetone and copper nitrate retained remarkable values of surface areas and pore volumes after the reduction treatment. Finally, outstanding values of metal dispersion, function of the temperature of the reduction, were obtained.

On account of the aforementioned remarkable properties, the catalysts obtained by the route a, figure 6.4 offered the best catalytic results in terms of methanol conversion, H_2 yield, and lower amount of secondary products. These results were also very satisfying compared with the one reported in literature considering the lower amount of copper and considering the absence of a promoter.

A hydrolytic sol-gel procedure was also proposed by Algorabi et al. [55] for the preparation of Cu-ZrO_2 catalysts for the hydrogenation of furfural, Figure 6.5. The synthesis strategy adopted to obtain homogeneous gels called for the use of zirconium propoxide diluted in isopropyl alcohol and ethylacetoacetate as a complexing. Copper (II) nitrate trihydrate is added to the reaction mixture maintained at 60 °C until gelation. Cu/ZrO_2 sol-gel catalysts loading 4%, 12%, and 16% were prepared using this protocol. Crystallisation of tetragonal zirconia was observed in all samples but only for low copper contents a shift towards higher theta degrees was detected, indicating a certain isomorphic substitution of Zr^{4+} by Cu^{2+}. Evidence of the homogeneous nature of catalysts obtained from alkoxide-based sol-gel chemistry is provided by X-ray Photoelectron Spectroscopy (XPS) investigations. The authors speculate that the peak at 935.1 eV can be attributed to strongly interacting Cu^{2+}-O-Zr species.

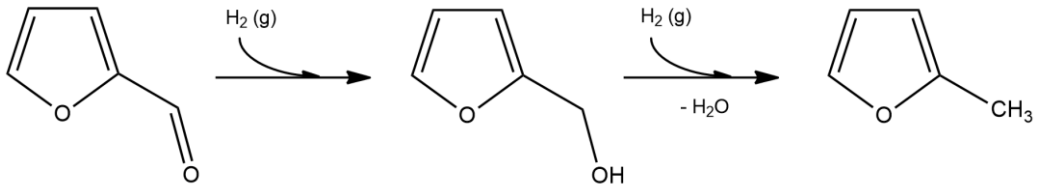

Furfural Furfuryl Alcohol 2-Methylfuran

Figure 6.5 Schematic representation of hydrogenation of furfural.

The results of the catalytic activity were very promising, although they revealed that the stability of the catalyst might be a matter of concern that deserves in-depth investigation. Indeed, the characterisation of the post-reaction materials showed a significant change in textural properties that could be the cause of the decrease in activity with reuse.

Despite being less versatile than the alkoxide route, Pechini method may be the right strategy to make preparation less expensive, using non-toxic products, and more environmentally friendly. In the work of Majedi et al. [65], zirconium acetate was used as a zirconium precursor, while lemon juice extracted from lemon (*Citrus aurantifolia*) fruits was used as a source of organic α-hydroxycarboxylic acid with the function of a metal chelating agent. The polymer resin was obtained by polyesterification with ethylene glycol (EG) after reaction at 90 °C for 3h. The authors also reported a successful attempt to limit particle aggregation phenomena with the use of a natural additive, sucrose. Structural and morphological characterizations of the samples revealed that zirconia crystallizes in its cubic phase with unit cell distortion from doping with Mg^{2+} and Ca^{2+} ions contained in lemon juice. The green method presented by the authors is certainly appealing and could be explored to prepare transition metal supported catalysts on zirconia.

6.3 Reverse micelle approach for photocatalysts

A major global concern affecting the environment and human health is climate change, mainly caused by the excessive use of fossil fuels and the release of CO_2. Simultaneously, human activities, agricultural production and growing population pressure all contribute to increasing levels of air and water pollution.

On account of its low-cost, versatility and environmental friendliness, photocatalysis is considered one of the most promising green chemistry technologies to address environmental concerns [66,67].

However, in order to look optimistically at photocatalysis and envisage it as a leading technology in the chemical industry, further investigations are needed to resolve some crucial aspects that limit the scale-up of the laboratory experiment. One of the main shortcoming lies in the low quantum efficiency of existing photocatalysts. Among semiconductors, TiO_2 undoubtedly presents numerous advantages, as widely reported in the literature, in terms of low cost, durability and long-term photostability [68]. However, only about 4 per cent of the solar spectrum can be exploited with TiO_2 catalysts, due to a relatively high band gap (about 3.2 per anatase) which precludes the adsorption of visible light.

Furthermore, the high recombination rate of photogenerated electron-hole pairs on the semiconductor surface may further limit its photocatalytic activity. A possible strategy for increasing the efficiency of photocatalytic activity is the doping of the TiO_2 lattice with heteroatoms [69].

The nature of the dopant, their concentration and the different positions in the TiO_2 lattice, whether interstitial or substitutional, can have a different impact on semiconductor properties. Transition metals are often used as dopants in semiconductors to improve the optical response and harvesting efficiency of visible light, inducing the formation of band gap states and promoting the formation of oxygen vacancies [70].

In this scenario, it is extremely relevant to have a synthesis method enabling the chemical-physical properties of the catalyst to be shaped through surface engineering strategies.

Among the different types of wet chemical processes, the reverse micelle approach is particularly effective in controlling the nucleation and growth of nanoparticles (NPs), while improving dopant dispersion. This is achieved by channelling reactions that usually take place in aqueous media into the small domains of reverse micelles, Figure 6.6.

The aqueous core of these micelles can be regarded as an ideal reactor boosting intimate contact between the precursors, achieving homogeneity and mixing on an atomic scale and ultimately promoting the inclusion

of the dopant in the titania lattice [71, 72]. In addition, the use of the reverse micelle approach can be seen as a valuable alternative to traditional procedures where the use of complexing agents is mandatory to avoid uncontrolled precipitation. Outstanding values of surface area can be also achieved by water-in-oil microemulsion compared to conventional methods.

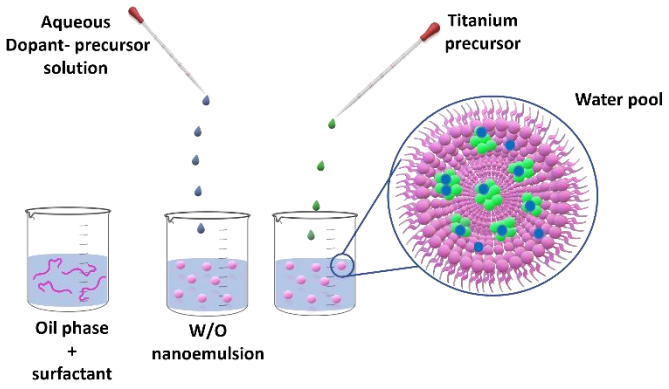

Figure 6.6 Synthesis of doped titania by reverse micelles approach

The textural properties of the photocatalyst play a decisive role in improving the adsorption/desorption mechanism with the selected pollutant molecule by contributing to improved photocatalytic performance. Varma et al. [73] prepared a series of Cu-TiO_2 samples with varying copper content (0.25, 0.5, 0.75, 1 wt%) using inverse micelle nanodomains where the oil phase consists of triton X-114 in hexane-toluene mixture (7:3 volume ratio).

They found improved properties compared to Cu-TiO_2 nanomaterials obtained by conventional sol-gel methods. In particular, the crystallite size of the Cu-TiO_2 samples was much smaller, the surface area increased consistently with 0.5 wt. % of copper, and the absorption wavelength was shifted towards visible light with the increased doping of Cu on TiO_2. The sample with 0.5 wt% copper proved to be the most efficient in degrading levofloxacin (LFX) under a 40 W visible LED light source. Higher copper contents favour the formation of Cu-LFX complexes, worsening the performance of the photocatalysts [73].

A cage-like environment for the preparation of manganese-doped titania was obtained employing polyoxyethylene (20) oleylether (Brij O20) as surfactant and cyclohexane as the oil phase [71]. 97% titanium(IV)butoxide (Ti-$(BuO)_4$) and manganese(II) nitrate tetrahydrate were used as precursors. The use of the reverse micelle method resulted to be extremely effective in increasing the dispersion of manganese both in bulk and on the titania surface. Furthermore, considering the ionic radii of Mn^{4+} and Ti^{4+}(octahedral Ti^{4+} r = 0.605 Å, octahedral Mn^{4+} = 0.53 Å), the progressive shrinkage of the unit cell as the manganese content increases evidenced the success of the preparation method in promoting substitutional doping [71].

Of all possible alternative to titania, cerium oxide has gained increasing attention as a photocatalyst due to its photochemical stability, 'cost-effectiveness' and 'eco-friendliness', and above all its peculiar redox chemistry. Indeed, cerium's unique ability to switch from the Ce(III) to the Ce(IV) state generates a strong catalytic potential due to high oxygen mobility in the CeO_2 lattice, without any structural modification of the fluorite structure. Moreover, titanium has been added to the list of critical raw materials since 2020 in UE justifying the urgent need for implementation of strategies toward new catalytic formulation [74].

Modification in size, shape and defects can be controlled by varying the synthesis conditions, in particular the type and nature of surfactant and the water/surfactant ratio. Reaction time and aging can be also investigated as impact factors on crystal growth and crystallinity [75].

The authors of Ref. 23 observed that textural and optical properties can be shaped by using non-ionic surfactants (Triton-x type) of different polar tail lengths. Indeed, the surface area increases significantly as the length of the polar tail increases, the particle size varies in relation to the radius of the aqueous centre, and the bad-gap decreases.

References

1. Y. I. Park, J. D. Kim and M. Nagai, Proton conductivity in sol-gel derived silicophosphate-PMA (PWA) glasses. J. Mater. Sci. Lett., 2000, 19, 2251-2253.
2. C. Wang, M. Nogami and Y. Abe, Protonic Conduction in P_2O_5-SiO_2 Glasses Prepared by Sol-Gel Method J. Sol-Gel Sci. Technol., 1999, 14, 273-279.
3. M. Nogami, C. Wang and Y. Abe, Fast proton conducting P_2O_5-SiO_2 glasses, in Proc. XVIII Cong. On Glass, ACS, San-Francisco, 1998, vol. D3, pp. 139–144.
4. M. Nogami, R. Nagao, C. Wang and Y. Abe, Role of Water on Fast Proton Conduction in Sol-Gel Glasses. J. Sol-Gel Sci. Technol., 1998, 13, 933-936.
5. N.J. Clayden, S. Esposito, P. Pernice, A. Aronne, Solid state ^{1}H NMR study, humidity sensitivity and protonic conduction of gel derived phosphosilicate glasses. J. Mater. Chem. 2002, 12, 3746–3753.
6. N.J. Clayden, S. Esposito, A. Aronne. Chemical heterogeneity in phosphosilicate gels by NMR magnetisation exchange. J. Chem. Soc. Dalton Trans. 2001, 2003–2008.
7. S. Esposito, N.J. Clayden, S.P. Cottrell, "Muon spin relaxation study of phosphosilicate gels", Solid State Ionics 2000, 348, Article number 115287.
8. A. Styskalik, D. Skoda, Z. Moravec, J. G. Abbott, C.E. Barnes, J. Pinkas, Synthesis of homogeneous silicophosphate xerogels by non-hydrolytic condensation reactions. Micropor. Mesopor. Mat. 2014, 197, 204–212.
9. N.J. Clayden, S. Esposito, P. Pernice, A. Aronne, Solid state ^{29}Si and ^{31}P NMR study of gel derived phosphosilicate glasses. J. Mater. Chem., 2001, 11, 936-943.
10. N.J. Clayden, A. Aronne, S. Esposito, P. Pernice, Solid state NMR study of phosphosilicate gels. J. Non-Cryst. Solids 2004, 345&346, 601–604.
11. Y. Choi, D. S. Park, H. J. Yun, J. Baek, D. Yun, J. Yi, Mesoporous Siliconiobium Phosphate as a Pure Brønsted Acid Catalyst with Excellent Performance for the Dehydration of Glycerol to Acrolein. ChemSusChem 2012, 5, 2460 – 2468.
12. G. Busca, Acid catalysts in industrial hydrocarbon chemistry. Chem. Rev. 2007, 107, 5366–5410.
13. N. Mansir, Y.H. Taufiq-Yap, U. Rashid, I.M. Lokman, Investigation of heterogeneous solid acid catalyst performance on low grade feedstocks for biodiesel production: A review. Energy Convers. Manag. 2017, 141, 171–182.
14. K. Shimizua. A. Satsuma, Toward a rational control of solid acid catalysis for green synthesis and biomass conversion. Energy Environ. Sci., 2011, 4, 3140-3153.
15. S. Esposito, "Traditional" Sol-Gel Chemistry as a Powerful Tool for the Preparation of Supported Metal and Metal Oxide Catalysts. Materials (Basel) 2019, 12, 668.
16. J. Livage, P.Barboux, M.T.Vandenborre, C. Schmutz, F. Taulelle, Sol-gel synthesis of phosphates. J. Non-Cryst. Solids 1992, 147–148, 18–23.
17. J.C. Schrotter, A. Cardenas, M. Smaihi, N. Hovnanian, Silicon and phosphorus alkoxide mixture: sol-gel study by spectroscopy technics. J. Sol-Gel Sci. Technol. 1995, 4, 195–204.
18. M. D'Apuzzo, A. Aronne, S. Esposito, P. Pernice, Sol-gel synthesis of humidity-sensitive P2O5–SiO2 amorphous films. J. Sol-Gel Sci. Technol. 2000, 17, 247–254.
19. S. C. Santos, L. S. Barreto, E. A. dos Santos, Nanocrystalline apatite formation on bioactive glass in a sol–gel synthesis. J. Non-Cryst. Solids 2016, 439, 30–37.
20. J.C. Schrotter, A. Cardenas, M. Smaihi, N. Hovnanian, Silicon and phosphorus alkoxide mixture: sol-gel study by spectroscopy technics. J. Sol-Gel Sci. Technol. 1995, 4, 195–204.
21. S.P. Szu, L.C. Klein, M. Greenblatt, Effect of precursors on the structure of posphosilicate gels: 29Si and ^{31}P MAS-NMR study. J. Non-Cryst. Solids 1992, 143, 21–30.
22. A. Matsuda, T. Kanzaki, Y. Kotani, M. Tatsumisago, T. Minami, Proton conductivity and structure of phosphosilicate gels derived from tetraethoxysilane and phosphoric acid or triethylphosphate. Solid State Ionics 2001, 139, 113–119.
23. S.C. Santos, L.S. Barreto, E. A. dos Santos, Nanocrystalline apatite formation on bioactive glass in a sol–gel synthesis. J. Non-Cryst. Solids 2016, 439, 30–37.

24. P. Malik, M. Awasthi, S. Sinha, Biomass-based gaseous fuel for hybrid renewable energy systems: An overview and future research opportunities. Int J Energy Res. 2021, 45, 3464–3494.
25. W. Dessie, X. Luo, M. Wang, L. Feng, Y. Liao, Z. Wang, Z. Yong, Z. Qin, Current advances on waste biomass transformation into value-added products. Applied Microbiology and Biotechnology 2020, 104, 4757–4770.
26. A. Hijazi, N. Khalaf, W. Kwapinski, J. J. Leahy, Catalytic valorisation of biomass levulinic acid into gamma valerolactone using formic acid as a H2 donor: a critical review. RSC Adv. 2022, 12, 13673–13694.
27. H. C. Genuino, H H. van de Bovenkamp, E. Wilbers, J. G. M. Winkelman, A. Goryachev, J. P. Hofmann, E. J. M. Hensen, B. M. Weckhuysen, P. C. A. Bruijnincx, H. J. Heeres, Catalytic Hydrogenation of Renewable Levulinic Acid to γ-Valerolactone: Insights into the Influence of Feed Impurities on Catalyst Performance in Batch and Flow Reactors. ACS Sustainable Chem. Eng. 2020, 8, 15, 5903–5919.
28. F. Kerkel, M. Markiewicz, S. Stolte, E. Müllerca, Werner Kunz, The green platform molecule gamma-valerolactone – ecotoxicity, biodegradability, solvent properties, and potential applications. Green Chem. 2021, 23, 2962-2976.
29. S. Esposito, B. Silvestri, C. Rossano, V. Vermile, C. Imparato, M. Manzoli, B. Bonelli, V. Russo, Eric M. Gaigneaux, A. Aronne, M. Di Serio, The role of metallic and acid sites of Ru-Nb-Si catalysts in the transformation of levulinic acid to γ-valerolactone. Applied Catalysis B: Environmental 2022, 310, 121340.
30. A.M.R. Galletti, C. Antonetti, V. De Luise, M. Martinelli, A sustainable process for the production of γ-valerolactone by hydrogenation of biomass-derived levulinic acid, Green Chem. 2012, 14, 688–694.
31. L. Minieri, S. Esposito, V. Russo, B. Bonelli, M. Di Serio, B. Silvestri, A. Vergara, A. Aronne, A Sol–Gel Ruthenium–Niobium–Silicon Mixed-Oxide Bifunctional Catalyst for the Hydrogenation of Levulinic Acid in the Aqueous Phase. ChemCatChem 2017, 9, 1 – 12.
32. P. Sun, X. Long, H. He, C. Xia, F. Li, Conversion of Cellulose into Isosorbide over Bifunctional Ruthenium Nanoparticles Supported on Niobium Phosphate ChemSusChem 2013, 6, 2190 – 2197.
33. R. Bechara, D. Balloy, J.Y. Dauphin, J. Grimblot, Influence of the Characteristics of γ-Aluminas on the Dispersion and the Reducibility of Supported Cobalt Catalysts. Chem. Mater. 1999, 11, 7, 1703–1711.
34. B. Puértolas, A. Smith, I. Vázquez, A. Dejoz, A. Moragues, T. Garcia, B. Solsona, The different catalytic behaviour in the propane total oxidation of cobalt and manganese oxides prepared by a wet combustion procedure. Chem. Eng. J. 2013, 229, 547–558.
35. R. Montero-Montoya, R. López-Vargas, O. Arellano-Aguilar, Volatile Organic Compounds in Air: Sources, Distribution, Exposure and Associated Illnesses in Children. Annals of Global Health 2018, 84(2), 225–238.
36. L.F. Liotta, G. Di Carlo, G. Pantaleo, A.M. Venezia, G. Deganello, Co_3O_4/CeO_2 composite oxides for methane emissions abatement: relationship between Co_3O_4–CeO_2 interaction and catalytic activity, Appl. Catal. B 2006, 66, 217–227.
37. T. García, B. Solsona, S.H. Taylor, Naphthalene total oxidation over metal oxide catalysts, Appl. Catal. B 2006, 66, 92–96.
38. S. Iravani, R. S. Varma, Sustainable synthesis of cobalt and cobalt oxide nanoparticles and their catalytic and biomedical applications. Green Chem. 2020, 22, 2643-2661.
39. S. Esposito, B. Bonelli, M. Armandi, E. Garrone, G. Saracco, Nanoparticles of CoAPO-5: synthesis and comparison with microcrystalline samples. Phys. Chem. Chem. Phys., 2015,17, 10774-10780.
40. R.P. Wang, M. J. Huang, A. Hariki, J. Okamoto, H.Y. Huang, A. Singh, D.J. Huang, P. Nagel, S. Schuppler, T. Haarman, B. Liu, F.M. F. de Groot, Analyzing the Local Electronic Structure of Co3O4 Using 2p3d Resonant Inelastic X-ray Scattering. J. Phys. Chem. C 2022, 126, 8752−8759.
41. B. Puértolas, A. Smith, I. Vázquez, A. Dejoz, A. Moragues, T. Garcia, B. Solsona, The different catalytic behaviour in the propane total oxidation of cobalt and manganese oxides prepared by a wet combustion procedure. Chemical Engineering Journal 229 (2013) 547–558.
42. I. Rossetti, B. Bonelli, G. Ramis, E. Bahadori, R. Nasi, A. Aronne, S. Esposito, New Insights into the Role of the Synthesis Procedure on the Performance of Co-Based Catalysts for Ethanol Steam Reforming. Topics in Catalysis 2018, 61, 1734–1745.

43. D.A. Eurov, T.N. Rostovshchikova, M.I. Shilin, D.A. Kirilenko, M.V. Tomkovich, M.A. Yagovkina, O.V. Udalova, I.Y. Kaplin, I.A. Ivanin, D.A. Kurdyukov, Cobalt oxide decorated porous silica particles: Structure and activity relationship in the catalytic oxidation of carbon monoxide. Applied Surface Science 2022, 579, 152121.
44. A. Badruzzaman, A. Yuda, A. Ashok, A. Kumar, Recent advances in cobalt based heterogeneous catalysts for oxygen evolution reaction. Inorganica Chimica Acta 2020, 511, 119854.
45. H. Tüysüz, Y.J. Hwang, S.B. Khan, A.M. Asiri, P. Yang, Mesoporous Co_3O_4 as an electrocatalyst for water oxidation. Nano Research 2013, 6(1): 47–54.
46. G. Bagnasco, C. Cammarano, M. Turco, S. Esposito, A. Aronne, P. Pernice, TPR/TPO characterization of cobalt–silicon mixed oxide nanocomposites prepared by sol-gel. Thermochim. Acta 2008, 471, 51–54.
47. A.Y. Khodakov, Fischer–Tropsch synthesis: Relations between structure of cobalt catalysts and their catalytic performance. Catal. Today 2009, 144, 251–257.
48. G. Olguin, C. Yacou, Smart, S.; da Costa, J.C.D. Influence of surfactant alkyl length in functionalizing sol-gel derived microporous cobalt oxide silica. RSC Adv. 2014, 4, 40181–40187.
49. A. Blasi, G. Fiorenza, C. Freda, Steam reforming of biofuels for the production of hydrogen-rich gas. Membranes for Clean and Renewable Power Applications 2014, Pages 145-181. Woodhead Publishing Limited, 2014 10.1533/9780857098658.3.145
50. S. Anil, S. Indraja, R. Singh, S.Appari, B. Roy, A review on ethanol steam reforming for hydrogen production over Ni/Al_2O_3 and Ni/CeO_2 based catalyst powders. International Journal of Hydrogen Energy 2022, 47, 8177-8213.
51. A.M. Ranjekar, G.D. Yadav, Steam Reforming of Methanol for Hydrogen Production: A Critical Analysis of Catalysis, Processes, and Scope. Ind. Eng. Chem. Res. 2021, 60, 89−113.
52. S. Sá, H. Silva, L. Brandão, J.M. Sousa, A. Mendes, Catalysts for methanol steam reforming-A review. Appl. Catal. B. 2010, 99, 43-57.
53. S. Esposito, M. Turco, G. Bagnasco, C. Cammarano, P. Pernice, New Insight into the Preparation of Copper/Zirconia Catalysts by Sol-Gel Method. Appl. Catal. A 2011, 403, 128−135.
54. S. Esposito, M. Turco, G. Bagnasco, C. Cammarano, P. Pernice, A. Aronne, Highly dispersed sol–gel synthesized $Cu–ZrO_2$ materials as catalysts for oxidative steam reforming of methanol. Applied Catalysis A: General 2010, 372, 48–57
55. S. Algorabi, S. Akmaz, S. N. Koç, The investigation of hydrogenation behaviour of furfural over sol–gel prepared Cu/ZrO_2 catalysts. Journal of Sol-Gel Science and Technology 2020, 96, 47–55.
56. Y. Shao, T. Wang, K. Sun, Z. Zhang, L. Zhang, Q. Li, S. Zhang, G. Hu, X. Hu, Competition between acidic sites and hydrogenation sites in Cu/ZrO2 catalysts with different crystal phases for conversion of biomass-derived organics. Green Energy & Environment 2021, 6, 557-566.
57. J. Livage, Inorganic Materials, Sol–Gel Synthesis of, in Encyclopedia of Materials: Science and Technology (Second Edition) 2001, 4105-4107.
58. I. Milošev, B. Kapun, P. Rodic, J. Iskra, Hybrid sol–gel coating agents based on zirconium (IV) propoxide and epoxysilane. J Sol-Gel Sci Technol 2015, 74, 447–459.
59. J. Livage, M. Henry, C. Sanchez, Sol-gel chemistry of transition metal oxides. Prog. Solid State Chem. 1988, 18, 259–341.
60. C. Sanchez, J. Livage,M. Henry, F. Babonneau, Chemical modification of alkoxide precursors. J. Non-Cryst. Solids 1988, 100, 65–76
61. M. Nabavi, S. Doeuff, C. Sanchez, J. Livage, Chemical modification of metal alkoxides by solvents: A way to control sol-gel chemistry. J. Non-Cryst. Solids 1990, 121, 31–34.
62. U. Schubert, Organically modified transition metal alkoxides: Chemical problems and structural issues on the way to materials syntheses. Acc. Chem. Res. 2007, 40, 730–737.
63. J. Livage, C. Sanchez, Sol-gel chemistry. J. Non-Cryst. Solids 1992, 145, 11–19.
64. H. Hayashi, H. Suzuki, S. Kaneko, Effect of chemical modification on hydrolysis and condensation reaction of zirconium alkoxide. J. Sol-Gel Sci. Technol. 1998, 12, 87–94.
65. A. Majedi, A. Abbasi, F. Davar, Green synthesis of zirconia nanoparticles using the modified Pechini method and characterization of its optical and electrical properties. Journal of Sol-Gel Science and Technology 2016, 77, 542–552.

66. D. Robert, N. Keller, E. Selli, Environmental photocatalysis and photochemistry for a sustainable world: a big challenge. Environ Sci Pollut Res 2017, 24, 12503–12505.
67. H. Wang, X. Li, X. Zhao, C. Li, X. Song, P. Zhang, P. Huo, X. Li, A review on heterogeneous photocatalysis for environmental remediation: From semiconductors to modification strategies. Chinese Journal of Catalysis 2022, 43 (2), Pages 178-214.
68. A. Fujishima, T. N.Rao, D.A. Tryk, Titanium dioxide photocatalysis. Journal of Photochemistry and Photobiology C: Photochemistry Reviews. 2000, 1 (1), 1-21.
69. A. Mancuso, N. Morante, M. De Carluccio, O. Sacco, L. Rizzo, M. Fontana, S. Esposito, V. Vaiano, D. Sannino, Solar driven photocatalysis using iron and chromium doped TiO_2 coupled to moving bed biofilm process for olive mill wastewater treatment. Chem. Eng. J. 2022, 450, 138107.
70. A. Khlyustova, N. Sirotkin, T. Kusova, A. Kraev, V. Titov , A. Agafonov, Doped TiO_2: the effect of doping elements on photocatalytic activity, Mater. Adv. 2020,1, 1193-1201.
71. B. Bonelli, O. Tammaro, F. Martinovic, R. Nasi, G. Dell'Agli, P. Rivolo, F. Giorgis, N. Ditaranto, F.A Deorsola, S. Esposito, Reverse Micelle Strategy for the Synthesis of MnOx−TiO_2 Active Catalysts for NH_3-Selective Catalytic Reduction of NOx at Both Low Temperature and Low Mn Content. ACS Omega 2021, 6, 24562−24574.
72. A Mancuso, O Sacco, V Vaiano, B Bonelli, S Esposito, F.S. Freyria, Nicola Blangetti, Diana Sannino Visible Light-Driven Photocatalytic Activity and Kinetics of Fe-Doped TiO_2 Prepared by a Three-Block Copolymer Templating Approach Materials 2021, 14 (11), 3105.
73. K.S. Varma, A.D. Shukla, R.J. Tayade, P.A. Joshi, A.K. Das, K.B. Modi, V.G. Gandhi, Photocatalytic performance and interaction mechanism of reverse micelle synthesized Cu-TiO2 nanomaterials towards levofloxacin under visible LED ligh. Photochemical & Photobiological Sciences 2022, 21, 77–89.
74. E. Lewicka, K. Guzik, K. Galos, On the Possibilities of Critical Raw Materials Production from the EU's Primary Sources. Resources 2021, 10, 50.
75. V. Uskokovic, M. Drofenic, Synthesis of materials with reverse micelles. Surface Review and Letters 2005, 12, 239-277.